

Research
Civil Engineering—Article

Preparation and Characterization of High-Strength Geopolymer Based on BH-1 Lunar Soil Simulant with Low Alkali Content



Siqi Zhou ^a, Chenghong Lu ^b, Xingyi Zhu ^b, Feng Li ^{a,*}

^a School of Transportation Science and Engineering, Beihang University, Beijing 100191, China

^b Key Laboratory of Road and Traffic Engineering of Ministry of Education, Tongji University, Shanghai 200092, China

ARTICLE INFO

Article history:

Received 15 June 2020

Revised 12 August 2020

Accepted 19 October 2020

Available online 29 December 2020

Keywords:

Space exploration

Lunar base

Geopolymer

Lunar soil simulant

Rheology

ABSTRACT

The construction of a lunar base and habitation on the Moon has always been on researchers' minds. Building materials used in *in situ* lunar resources are of great significance for saving expensive space freight. In this study, a new type of lunar soil simulant named Beihang (BH)-1 was developed. The chemical mineral composition and microstructure of BH-1 closely resemble those of real lunar soil, as verified by X-ray fluorescence spectroscopy (XRF), X-ray diffraction (XRD), scanning electron microscopy (SEM), and reflectance spectra. This research also synthesized a geopolymer based on BH-1 cured at simulated lunar atmospheric conditions. We also investigated the effect of supplementing aluminum (Al) sources on the enhancement of geopolymer strength based on BH-1. The rheological behavior of alkali-activated BH-1 pastes was determined for workability. XRF, XRD, Fourier transform infrared spectroscopy, SEM coupled with energy dispersive spectroscopy, and ²⁷Al magic angle spinning-nuclear magnetic resonance were used to characterize resulting geopolymers. Rheological test findings showed that the rheology of BH-1 pastes fits the Herschel-Bulkley model, and they behaved like a shear-thinning fluid. The results showed that the 28-day compressive strength of the BH-1 geopolymer was improved by up to 100.8%. Meanwhile, the weight of additives required to produce per unit strength decreased, significantly reducing the mass of materials transported from the Earth for the construction of lunar infrastructure and saving space transportation costs. Microscopic analyses showed that the mechanism to improve the mechanical properties of the BH-1 geopolymer by adding an additional Al source enhances the replacement of silicon atoms by Al atoms in the silicon-oxygen group and generates a more complete and dense amorphous gel structure.

© 2020 THE AUTHORS. Published by Elsevier LTD on behalf of Chinese Academy of Engineering and Higher Education Press Limited Company. This is an open access article under the CC BY-NC-ND license (<http://creativecommons.org/licenses/by-nc-nd/4.0/>).

1. Introduction

The Moon is the nearest celestial body to the Earth. Its unique space environment and abundant mineral resources make the Moon a key transit station for deep space exploration missions [1]. At present, landing on the Moon to exploit lunar resources and building a Moon base have become the focus of competition among major and emerging aerospace countries. As early as 1972, a 12-man lunar colony, as earth independent as possible, was proposed by the the American Society for Engineering Education (ASEE) Engineering Systems Design Institute and the University of Houston to use lunar resources [2]. China will fulfill the

dream of the human-crewed lunar landing and lunar base establishment after 2020 [3].

1.1. Lunar environment

The Moon's environment differs from Earth in many ways. On the Moon, the most obvious environmental factors that concern researchers working on lunar base construction for the possibility of endangering human existence are extreme temperature, intense radiation, and the absence of any atmosphere. Lunar infrastructure construction is crucial to improve the lunar base's safety, functionality, and operational efficiency.

The temperature on the Moon is between −233 and 125 °C, and its surface temperature varies significantly from day to night (a day and night on the moon is about equal to a month on the Earth) because there is no atmospheric heat transfer. Since the Moon

* Corresponding author.

E-mail address: lifeng98@buaa.edu.cn (F. Li).

has very low thermal inertia on its own, its surface temperature during the day depends primarily on absorbing solar radiation. At the lunar equator, the full moon absorbs solar radiation to produce a lunar temperature of 123 °C and the temperature decreases with increasing latitude.

Meteoroids are another safety challenge. Micrometeoroids, with a mass of approximately milligrams mass, are expected to hit lunar installations and equipment almost every year. Meteorites with a mass of 10^{-6} g can form impact craters on the Moon with a diameter of up to 500 μm . The largest recorded impacts were produced by meteoroids of approximately 5 t in July 1972 and May 1975 [4]. In all, seven meteoroid impacts of 1 t or more were observed from 1972 to 1977 during lunar seismic monitoring [4]. Major meteoroids are sporadic, but their effects can be devastating. For instance, landslides and slumping of crater walls may be triggered seismically by impacts. Thus, the main challenge faced by many researchers is building a high-strength moon shelter.

Radiation on the Moon surface is mainly attributed to solar, galactic, and human-made radiation [5]. Human-made radiation, such as the possibility of using radioactive sources of energy, is easily mitigated and, in any case, is not a problem. However, solar and galactic radiation are far more severe and challenging to address. Solar radiation in the form of solar energetic particles (SEPs) containing particles of over 10 MeV and larger than $3 \times 10^7 \text{ cm}^{-2}$ can be unpredictable and harmful to astronauts' health. High-energy protons in solar radiation cause a single particle effect that could damage lunar probes' electronic components. These high-energy protons also ionize the optical material, causing the optical device to break down. If a lunar colony exists for a long time, it can be assumed that there will be at least one major solar event. Thus, it is necessary to prepare for radiation shielding.

As for transportation, the Moon has low gravity, a rugged surface, and floating dust [4], making it difficult for lunar rovers to travel. High-velocity and volcanism have been the two main factors controlling the Moon's terrain [4]. The mare basins are rimmed with high mountains formed during the impact of planetesimals; many of these basins were smoothed when filled or partly filled with basaltic lavas. Deep channels cut the mare surfaces, and faults and wrinkle ridges buckle those same surfaces. Floating dust on the Moon's surface easily adheres to the lunar rovers' solar panel, leading to equipment failure. Apollo 15 lunar rover's maximum speed is only 13 $\text{km}\cdot\text{h}^{-1}$ [6], and the maximum speed of the Yutu lunar rover in China is only 0.2 $\text{km}\cdot\text{h}^{-1}$ [7]. The construction of lunar roads on hard surfaces can effectively improve speed and safety of transportation of lunar equipment, further enhancing the efficiency with which people and goods are transported, resulting in improved lunar scientific research activities.

1.2. Lunar infrastructure construction using local resources

The Moon is indeed an alien environment. While these differences may seem harsh for human survival, it is crucial to consider that some of the differences also provide unique opportunities for using the lunar environment and its resources in future space exploration. Considering the difficulty and high cost of carrying large-payload materials from the Earth to the Moon, it is crucial to produce building materials using the resources available on the Moon [8,9].

In-situ resource utilization (ISRU) technology has become a popular research topic in lunar construction [10]. Nearly all of lunar surface is covered with several loose regolith meters, also known as lunar soil. Researchers worldwide use various technical routes to produce building materials from lunar soil. Some researchers have used sulfur-rich lunar soil to produce sulfur concrete [11], which involves melting sulfur and aggregates. Although

this method solves the issue of sourcing raw materials, it has several drawbacks, mostly the limited working temperature of sulfur. Sulfur concrete melts and deforms when the temperature reaches 119 °C, while the maximum temperature on the lunar surface can reach 125 °C [12], which significantly limits the application of sulfur concrete. In addition, the low durability of thermal cycles also limits the application of sulfur concrete on the Moon.

Basaltic regolith is readily available on the Moon. Dalton and Hohmann [2] proposed a method to produce building material by melting Moon basalt at 1300–1350 °C and pouring it into a drum to crystallize, with temperatures and pressures carefully controlled. The cast basalt was then poured into precast molds. An issue with cast basalt is the shrinkage during cooling, leading to unavoidable cracks. Another problem is that the cast basalt is hard and fragile and thus cutting and drilling are almost impossible [13].

Another method is to use a high-temperature beam by focusing sunlight and solidifying lunar soil, which can be used to pave the lunar surface [14]. However, the thermal stress inside the material will lead to the deformation of the lunar soil plate, which is not desired for use in full-scale pavement construction.

1.3. Summary of lunar soil simulants

The lunar soil brought back by the Apollo project spacecraft is very limited for research purposes. ISRU technology studies on lunar base construction require a large amount of lunar soil for experiments. Therefore, it is necessary to produce lunar soil simulants using Earth materials. Researchers worldwide have been working on the preparation of lunar soil simulants. At present, the typical lunar soil simulants include Johnson Space Center (JSC)-1, Minnesota lunar simulant (MLS)-1, Fuji Japanese Simulant (FJK)-1, Chinese Academy of Sciences (CAS)-1, and Tongji (TJ)-1 [15].

It is well known, yet not fully appreciated, that "one-of-a-kind lunar simulant does not fit all needs" [15]. Different types of lunar soil simulants have been developed for specific applications, including the duplication of geotechnical properties and chemical or mineralogical analogues. For example, the first lunar soil simulant, JSC, highly similar to real lunar soil in terms of geotechnical properties, was developed by Dr. David Carrier at the JSC for drilling research. However, this soil simulant was completely incorrect with regard to lunar mineralogy, composition, particle size distribution, and so forth.

In 1993, JSC-1 was designed as glass-rich basaltic ash, which approximates the bulk chemical composition and mineralogy of [16]. It should be noted that soil in different regions of the Moon usually varies significantly in chemical and mineral composition, and particle size distribution. As a result, it becomes crucial to declare which part of the Moon the lunar soil simulant's reference substance is from, which is ambiguous in many studies [16].

Some researchers have focused on the similarity in a particular composition. For example, it became apparent that the titanium dioxide (TiO_2) content in lunar soil samples returned with Apollo 11 was too high (> 20 wt%). MLS-1 [17] used basalt from a quarry in Duluth, USA, which was one of the highest TiO_2 contents on Earth as source material. The main characteristics of other typical lunar soil simulants are summarized in Table 1 [15–20].

1.4. Synthesis of geopolymer with lunar soil simulants

Other studies have found that lunar soil is an inorganic mineral material rich in silica and aluminum (Al) [12]. In recent years, with the in-depth research on the properties and reaction mechanism of geopolymer materials, a new scheme has been developed to produce lunar building materials, which synthesizes a geopolymer using lunar soil.

A geopolymer is a new type of inorganic high polymeric cementitious material discovered by Davidovits in the 1980s [21]; it is an

Table 1
Summary of typical lunar soil simulants.

Lunar soil simulant	Country	Year	Application	Advantage	Disadvantage
JSC [15]	United States	1971	Drilling research	Excellent duplication of geotechnical properties High TiO ₂ content	Tremendously different composition compared with anything lunar Not to have correct mineralogy, chemistry, or engineering properties
MLS-1 [17]	United States	1990	Studies of materials where titanium has a major impact	Available in large scale	Ambiguous chemical or mineralogical analog
JSC-1 [16]	United States	1993	Large- and medium-scale engineering studies	Excellent duplication of chemistry and mineralogy	Acceptable median grain size but without considering particle size distribution
CAS-1 [18]	China	2009	Geopolymer synthesis	Close resemblance to the soil from the Maria geological terrain of the Moon	Ambiguous particle size
JSC-1A [19]	United States	2010	Developing glass and ceramic materials	Similar particle size distribution with lunar soil 14163	Lack of mineral composition analysis
Korea lunar stimulant (KLS)-1 [20]	Republic of Korea	2018	Geotechnical engineering		

aluminosilicate material with a covalently bonded polymer structure synthesized by alkali activation of precursor materials rich in silicon (Si) and Al. Compared with ordinary Portland cement, it has the advantages of high mechanical strength [22], high and low temperature resistance [23], radiation resistance [12], freezing and thawing resistance [24], improved durability [25], and low shrinkage [26]. In addition, the possible presence of water and ice [27] in the lunar polar region can also provide the water molecules required for geopolymerization. Therefore, it is feasible to use geopolymer technology for lunar base construction.

Researchers worldwide have been using lunar soil simulants to prepare geopolymers. Montes et al. [12] used the JSC-1A lunar soil simulant to prepare a geopolymer. The material proved to have the ability to resist radiation. Wang et al. [28] used volcanic ash from Cameroon to prepare a lunar soil simulant and studied the freezing and thawing resistance of geopolymers. Pilehvar et al. [29] used urea as a superplasticizer for 3D printing based on lunar geopolymer mixtures. The preparation of geopolymers from lunar soil simulants has become a research hotspot in lunar base construction.

However, there are still some challenges in the preparation of geopolymers from lunar soil. One of the most significant challenges is the low mechanical strength resulting from the coarse particle size of lunar soil. Lunar soil has a mean particle size between 42 and 105 μm . The mean particle size of lunar soil collected by Apollo 14 was 802 μm [30]. The resulting geopolymers were below 20 MPa [12,28,29], which is strong enough as building material to protect against meteoroids on the Moon. Second, in previous studies, the experimental conditions did not simulate lunar temperatures [12,28,29]. Most specimens were cured at 25 °C or at a fixedly elevated temperature. The effect of the curing temperature on the mechanical strength of the geopolymer is significant. Taking advantage of the Moon's natural temperature environment to cure a geopolymer based on lunar soil will significantly reduce the cost by eliminating the need for a curing box or curing chamber.

Another problem is that Al is scarce in both lunar soil and its simulants. The mass fraction of alumina is less than 20%, while the alumina content in common geopolymer raw materials, such as F-grade fly ash, can be as high as 40% [31]. The molar ratio of Si and Al (Si/Al ratio) in the starting materials highly influences the strength development of geopolymers. In general, an Si/Al ratio of raw materials under two shows high pozzolanic activity for geopolymer preparation [32]. While the Si/Al ratio of the lunar soil is approximately four, the reactivity of lunar soil tends to be lower [32,33], which probably results in low mechanical strength of the lunar soil geopolymer.

1.5. Rheology of alkali-activated lunar soil simulant paste

In addition to enhancing mechanical strength, the further application of alkali-activated lunar soil as a grout or building material

also depends on the rheological properties of the new mix during pumping, injection, spreading, molding, and compaction. A rheological property refers to the deformation and flow properties of matter under the action of external forces. The quantitative relationship between the shear stress applied to the fluid and the shear rate varies with the viscosity of the fluid. Rheology is the study of the relationship between shear stress and shear rate in fluid flow; this relationship is known as the rheological properties of the fluid [34].

In the literature, very few investigations on the rheology of alkali-activated real lunar soil or simulants can be detected. Primary studies on the rheological behavior of alkali-activated geopolymer paste have been conducted on cement [35], fly ash [36], phosphorus slag [37], and metakaolin [38]. Fresh geopolymer paste is usually a heterogeneous mixture, most of which exhibits complex non-Newtonian fluid characteristics. Most researchers use the concept of plastic fluid to describe it. Currently, the most widely used model with the best adaptability is the Bingham model [39]. Although the Bingham model is mostly used for cementing material, some non-linearity has been observed; other models such as power-law [40], Casson [41], modified Bingham [42], and Herschel–Bulkley models [37] can be used to describe the rheological properties of geopolymer pastes.

The main rheological properties of geopolymer pastes analyzed by the rheological test model fitting include yield stress, flow index, and thixotropic parameter, which characterize workability, shear-thinning, shear-thickening behavior, and restorability after shearing [37]. Further, the open construction time can be obtained by further studying the relationship between these properties and time.

1.6. Aim and scope of this article

The objective of this study was to develop a new lunar soil simulant named Beihang (BH)-1 similar in chemical and mineral composition to real lunar soil and use it to synthesize high-strength geopolymer cured at simulating lunar temperature. The effect of supplementing an Al source on the enhancement of geopolymer strength based on BH-1 has been investigated. The rheological behavior of alkali-activated BH-1 pastes was also determined.

This paper is divided into four parts. The first part introduces studies on lunar base construction based on *in situ* lunar source use. The second part describes the experimental design, including raw material selection, paste preparation, and test methods. The third presents the results of this study. The fourth section presents the research findings, focusing on the three key themes: the similarity between BH-1 and real lunar soil, the effect of Al₂O₃ and metakaolin on the rheological behavior of fresh BH-1 paste and the mechanical strength of the resulting geopolymer, and the

strength enhancement mechanism of the lunar soil polymer by the Al source.

2. Experimental

2.1. Raw materials

As mentioned above, several studies have shown that the compressive strength of geopolymers fabricated from lunar soil simulants did not exceed 20 MPa, which may be attributed to the large size of lunar soil particles. The median particle size of lunar soil samples taken from almost all batches was over 74 μm . The median particle size of lunar soil samples collected by Apollo 14 was 800 μm [30]. The particle size distribution of the No. 71501 lunar soil sample brought back by Apollo 17, presented in Fig. 1 [30], shows that over 50% of the real lunar soil particles are larger than 74 μm , which is considered as the upper limit of geopolymer raw materials or cement-like binder material. This leads to a lower contact area between the alkaline activator and lunar soil particles, and therefore, slower geopolymerization. However, lunar soil has a high aluminosilicate content. Volcanic scoria with a composition similar to that of lunar soil is known to geopolymerize resulting materials with high compressive strength over 60 MPa [43]. Thus, it can be inferred that reducing the particle size may enhance geopolymerization reactivity, and the resulting materials may have high mechanical strength, improving the safety and reliability of the lunar shelter. Many other researchers have used the same method. Pilehvar et al. [29] used De NoArtri (DNA)-1 lunar soil simulant with a half-content diameter (d_{50}) of 43.55 μm . Alexiadis et al. [44] milled JSC-1A lunar soil simulant, with a mean particle size of 28 μm , and enhanced the compressive strength of the resulting geopolymer up to 18 MPa.

To test this hypothesis, volcanic scoria was mined, dried, crushed, and sieved to 74 μm to obtain a BH-1 lunar soil simulant and prepare the geopolymer. The volcanic scoria was mined from the Jinlongdingzi volcanic scoria cone located in Jinchuan Town, Huinan County, Jilin Province, China (42°21'N, 126°18'E). The origin of the raw materials was determined according to previous research results and preliminary comparative analyses of volcanic ash from different sources to find a material similar to lunar soil. Both the CAS-1 lunar soil simulant [23] developed by the Institute of Geochemistry of the Chinese Academy of Sciences and the Northeastern University (NEU)-1 lunar soil simulant [24] developed by Northeastern University were taken from the same location. The bulk density of the volcanic scoria sample tested by mercury intrusion porosimetry (MIP, AutoPore IV 9500, USA) is 1.6747 $\text{g}\cdot\text{cm}^{-3}$, which is within the range of the average lunar soil density 1.45–1.90 $\text{g}\cdot\text{cm}^{-3}$ [45]. A laser particle size analyzer (Mastersizer 2000, Malvern, UK) was used to analyze BH-1 lunar soil simulant particle size. The cumulative distribution curve of the particle size of BH-1 in Fig. 1 shows that the medium particle size (d_{50}) of BH-1 is 38.22 μm . Milling produced an eightfold reduction in the mean particle size of BH-1 compared with lunar soil brought by Apollo 17, as shown in Fig. 1.

Thus, BH-1 lunar regolith simulant was developed as a chemical and mineralogical analog to real lunar soil. Various tests, including X-ray diffraction (XRD), X-ray fluorescence (XRF), reflectance spectra, and scanning electron microscopy (SEM), were carried out to verify the chemical composition and mineral composition of BH-1 for comparison with real lunar soil (Section 2.3).

The alkali activator used in this study consisted of sodium hydroxide (NaOH) and industrial-grade sodium silicate. NaOH was analytically pure, with more than 99% effective component content by mass. Sodium silicate (SiO_2 : 25.3%–26.2% (wt); Na_2O : 7.5%–8.5% (wt)) with a density of 1.374 $\text{g}\cdot\text{mL}^{-1}$ had a water content

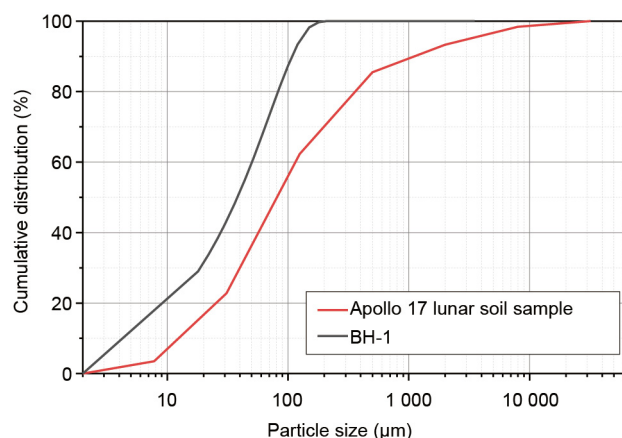


Fig. 1. Particle size distribution curves of BH-1 lunar soil simulant and real lunar soil collected by Apollo 17 [30].

of 65 wt%. Distilled water was adopted in this study to avoid the effect of impurity ions on the experimental results.

According to a previous study [46], geopolymers based on lunar soil have low mechanical strength owing to the lack of Al, and thus, a high Si/Al ratio in raw materials. In this study, metakaolin (Metamax, BASF, Germany) and alumina (Al_2O_3 , Beijing Chemical Works, China) were used as Al sources during geopolymerization. The XRD patterns of Metamax and analytical reagent (AR) Al_2O_3 are shown in Fig. 2. It can be observed that the XRD pattern of Metamax has no distinct diffraction peaks and shows a noticeable hump in the range of 20°–30° of 2θ , which indicates that Metamax is mainly composed of amorphous substances. In contrast, Al_2O_3 shows sharp diffraction peaks. The XRF analysis of Metamax is shown in Table 2. The d_{50} of Metamax is 3.87 μm , which is much smaller than BH-1. Aluminum in the form of oxide accounts for nearly half by mass, indicating that it is a suitable Al source.

2.2. Paste preparation

Using trial and error testing, the mass ratio of NaOH to BH-1 lunar soil simulant in the control group (Cg) was determined to be 9% and that of sodium silicate to BH-1 was 10%. On this basis, Al_2O_3 with mass ratios of 3%, 5%, and 10% to BH-1, and Metamax with mass ratios of 5% and 10% were added, respectively. The water mass was composed of water in sodium silicate and additional distilled water. The water–binder ratio was 0.28. The mass of NaOH, sodium silicate, Metamax, Al_2O_3 , and BH-1 are represented by m_{SH} , m_{SS} , m_{Kao} , m_{Al} , and m_{BH} . The specific mix design is shown in Table 3.

The NaOH solution was first prepared by mixing NaOH and distilled water according to the design proportion in the test runs. The NaOH solution was cooled to room temperature and was then mixed with sodium silicate to obtain an alkaline activator. The activator was cooled to room temperature and used after 24 h. The BH-1 geopolymer pastes were then generated by mixing BH-1, and an alkaline activator solution based on the test runs with a mortar mixer. The low-speed mixing lasted 120 s at a speed of (140 ± 5) $\text{r}\cdot\text{min}^{-1}$ before the high-speed mixing was processed for 120 s at a speed of (285 ± 10) $\text{r}\cdot\text{min}^{-1}$. A BH-1 geopolymer paste was prepared.

2.3. Test methods

Several tests were conducted to verify the similarity between the BH-1 lunar regolith simulant and lunar regolith, including XRD (D8 AdvanceX, Bruker, Germany), XRF (XRF-1800, Shimadzu,

Table 2
Chemical composition of metakaolin (Metamax) from BASF, Germany.

Composition	SiO ₂	Al ₂ O ₃	TiO ₂	Fe ₂ O ₃	Na ₂ O	MgO	K ₂ O	CaO	LOI
Content (wt%)	51.01	46.16	1.62	0.37	0.30	0.14	0.14	0.03	0.23

LOI: loss on ignition.

Japan), reflectance spectra with handheld visible-to-near-infrared (VNIR) spectroradiometer (HandHeld 2, ASD FieldSpec, UK), and SEM (SU8020, Hitachi, Japan). The results were compared with real lunar soil samples collected by the US Apollo project and lunar soil simulants prepared by other researchers to demonstrate the similarity between BH-1 and lunar soil.

The rheological behavior of alkali-activated BH-1 paste was determined by estimating the yield stress, flow index (n), and thinning index (TI). To investigate the effect of alkali activator on the rheological behavior of BH-1 paste, an additional paste group prepared using water and BH-1 simulated lunar soil was added to the test group in Table 3. The water-to-binder ratio was 0.28. This test group was named blank control group (blankCg). The test equipment was a rotational rheometer (MCR 702 MultiDrive, Anton Paar, Austria) at (25 ± 5) °C, and RheoCompass software (Anton Paar, Austria) was used for data evaluation. The measurements were performed in a FlexibleCupHolder system (Anton Paar,

Austria), on which a standard measuring cup of 42 mm diameter was mounted to store the samples. The measuring rotor was a ST30-4V-40 cylinder spindle with a diameter of 30 mm and a length of 40 mm. The experimental process consisted of a pre-shearing period of 120 s at 100 s^{-1} , with the shear rate increasing from 0 to 100 s^{-1} in 90 s, and then decreasing from 100 to 0 s^{-1} in 90 s, according to the American Society of Testing Materials (ASTM) standard D2196-18 [47]. Rheological parameters, including shear rate, shear stress, and apparent viscosity, were recorded once per second.

To prepare specimens for mechanical properties tests, the pastes were then molded into $40 \text{ mm} \times 40 \text{ mm} \times 160 \text{ mm}$ stainless steel triple molds, flattened with a scraper, and vibrated on the vibration table for 2 min to remove bubbles generated during the pouring process. After casting, the samples were cured at 20 °C for 24 h and demolded. Specimens were then packed with plastic wrap and cured at 20 °C until they were retrieved for testing. The curing temperature was determined by the bolometric brightness temperature captured with the Diviner Lunar Radiometer Experiment onboard the Lunar Reconnaissance Orbiter (LRO) [48]. According to a previous study [46], the mechanical strength of a geopolymer based on lunar soil simulant increases with curing temperature. In particular, the geopolymer from the lunar soil simulant could form 28-day compressive strength over 40 MPa under a curing temperature of 40 °C, while the highest 28-day compressive strength was only 18.5 MPa at 20 °C [46]. However, according to the surface temperature measured by Diviner [48] (Fig. 3), only the area between the equator and the latitude of 30° can reach temperatures above 40 °C, while the surface temperature at a latitude of 60° is maintained at approximately 20 °C over a long time range. Therefore, the curing temperature was set at 20 °C in this study to explore the enhancement effect of Al₂O₃ and Metamax on the mechanical strength of a geopolymer based on BH-1 at a lower temperature.

The flexural strength and compressive strength of hardened BH-1 specimens were tested according to the specifications of GB/T 17671-1999 at room temperature with Model TYE-3000 compression testing machine (Jianyi Instrument Machinery Co., Ltd., China); thereafter, the specimens were cured for 7 and 28 days according to the experimental settings, as shown in Figs. 4(b) and (c). Three specimens were tested for flexural strength in one test run with a loading rate of $(50 \pm 10) \text{ N}\cdot\text{s}^{-1}$. Six specimens were tested for compressive strength in one test run with a loading rate controlled at $(2400 \pm 200) \text{ N}\cdot\text{s}^{-1}$.

The resulting geopolymers of 28-day curing time were dried at 60 °C for 1 h and ground to a fine powder with particle sizes $\leq 75 \mu\text{m}$ for the microscopic test. XRD was conducted to analyze changes in the mineral composition. FTIR spectra were

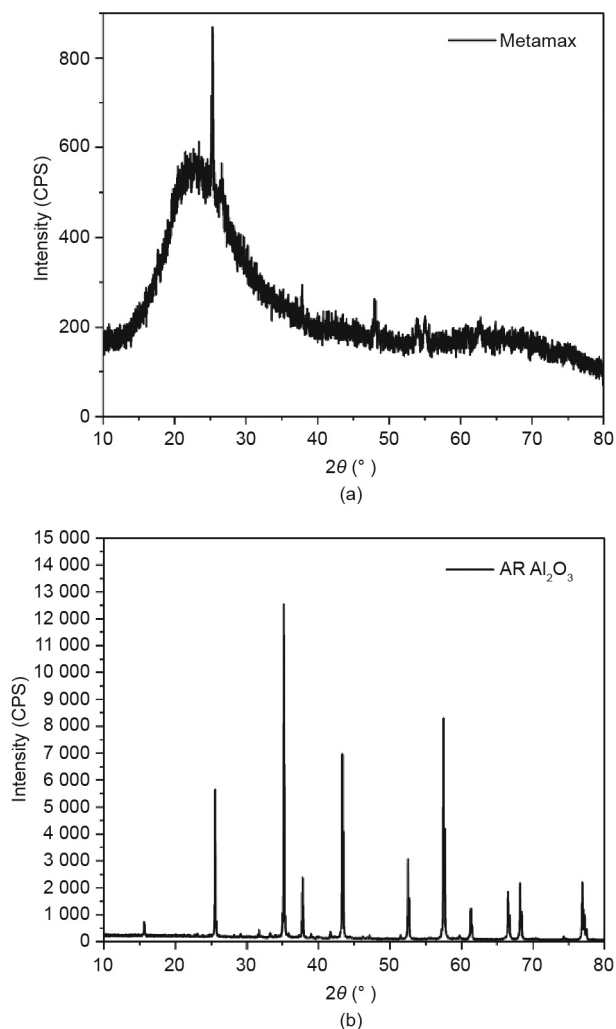


Fig. 2. XRD pattern of (a) Metamax and (b) AR Al₂O₃. CPS: counts per second; 2θ: scattering angle.

Table 3
Mix design.

Test No.	m_{SH}/m_{BH}	m_{SS}/m_{BH}	m_{Al}/m_{BH}	m_{Kao}/m_{BH}
Cg	9%	10%	—	—
Al3	9%	10%	3%	—
Al5	9%	10%	5%	—
Al10	9%	10%	10%	—
Kao5	9%	10%	—	5%
Kao10	9%	10%	—	10%

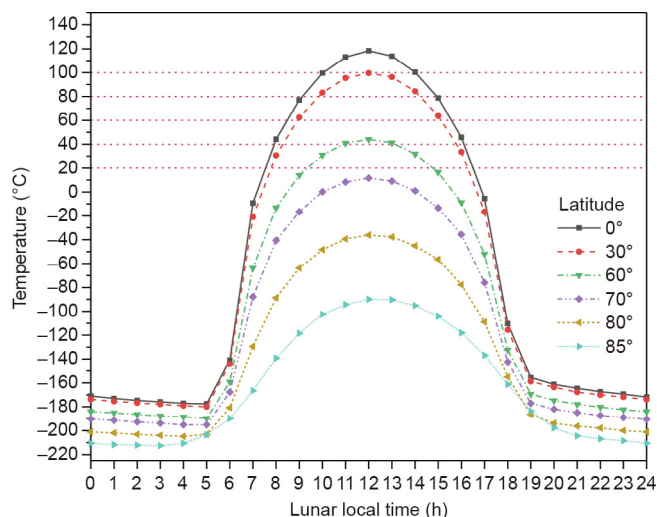


Fig. 3. Lunar surface temperature tested by Diviner. Reproduced from Ref. [48] with permission of Elsevier Ltd., ©2017.

recorded on a Nicolet IS10 Fourier infrared spectrometer using the KBr pellet method. ^{27}Al magic-angle spinning (MAS)-nuclear magnetic resonance spectroscopy (NMR) solid-state spectra were recorded at day 28 using a Bruker AVANCE III 600 M (Bruker BioSpin, Germany). The resonance frequency was set as 104.23 MHz with the probe rotating at 5 kHz. The pulse width was 1.9 s with a cycle time of 15 s. SEM–energy dispersive spectrometer (EDS) tests (SU8020, Hitachi, Japan) were conducted to analyze the morphology and elemental components of the BH-1 geopolymer.

3. Results and discussion

3.1. Characterization of BH-1 lunar regolith simulant

As mentioned above, it is difficult for a one-of-a-kind lunar soil simulant to fit all the characteristics of real lunar soil and all the engineering needs. The BH-1 lunar regolith simulant was developed as a mineralogical and chemical analog to real lunar soil brought back by Apollo 16. The mineral composition of BH-1 was analyzed by comparing the diffraction pattern with Powder Diffraction File (PDF) database maintained by the International Center for Diffraction Data [49], as shown in Fig. 5, and compared with the XRD pattern of the Apollo 16 sample [50]. The mineral

composition of BH-1 shows albite-high, andesine, anorthite, and labradorite as the main minerals. Anorthite matches the main mineral composition of the lunar soil sample from Apollo 16. Albite-high, andesine, and labradorite are the different minerals compared with Apollo 16 lunar soil samples. However, they all belong to the feldspar group, showing similar geopolymerization characteristics. The mineral composition of BH-1 was also been compared with other lunar soil simulants. As expected, the mineral components of BH-1 are very similar to those of both CAS-1 [18] and NEU-1 [51] lunar soil simulants, the major mineral component of which is anorthite, as they were collected from the same location. However, BH-1 has a different mineral composition than that of one of the most widely used lunar soil simulant JSC-1 [16], the mineral composition of which includes plagioclase, clinopyroxene, olivine, and opaque oxides with or without glass. A possible explanation for this might be that JSC-1 was developed referring to the lunar sample brought back by Apollo 14, while BH-1 is based on the Apollo 16 lunar soil sample. Different sampling sites lead to different mineral characteristics.

The primary oxide composition of the BH-1 lunar simulant characterized by XRF is shown in Table 4 with the data of lunar soil samples from Apollo 12, 14, 15, and 16 included for comparison [30]. The major oxide of BH-1 consists of SiO_2 , FeO , and Al_2O_3 , with a sum equal to 76.5 wt%. The $\text{SiO}_2/\text{Al}_2\text{O}_3$ molar ratio is 4.45 which is close to that of Apollo 16 lunar soil (5.44). The composition of lunar soil varies in different regions of the Moon. It can be concluded that the content of SiO_2 and Al_2O_3 in BH-1 is within the content range of Apollo samples, that is, 42.20%–48.10% (SiO_2) and 12.90%–17.40% (Al_2O_3). The Na_2O and K_2O contents are 3.8% and 3.3%, respectively. However, for all lunar soil samples, a low content below 1% of Na_2O and K_2O was observed, as shown in Table 4. Other lunar simulants (JSC-1 and CAS-1) also fail to match such low Na_2O and K_2O contents in real lunar soil. Considering that the main elements that affect geopolymer formation are Al and Si [12,44], this difference is acceptable. Another common feature in all lunar soil simulants is the low TiO_2 content, which was also reported by Taylor et al. [15]. Only the lunar soil sampled by Apollo 12 has a high TiO_2 content (7.80%); other lunar soil samples and lunar soil simulants have low TiO_2 content less than or equal to 3.00%. High titanium (Ti) lunar soil is unnecessary since Ti has little influence on the geopolymerization reaction.

In addition, reflectance spectra of lunar regolith vary greatly at different locations on the Moon surface, which can be an effective method to characterize lunar regolith. The reflectance spectral properties of mature soils from each of the Apollo sites [50], CAS-1, and BH-1 lunar soil simulants are dotted and compared,

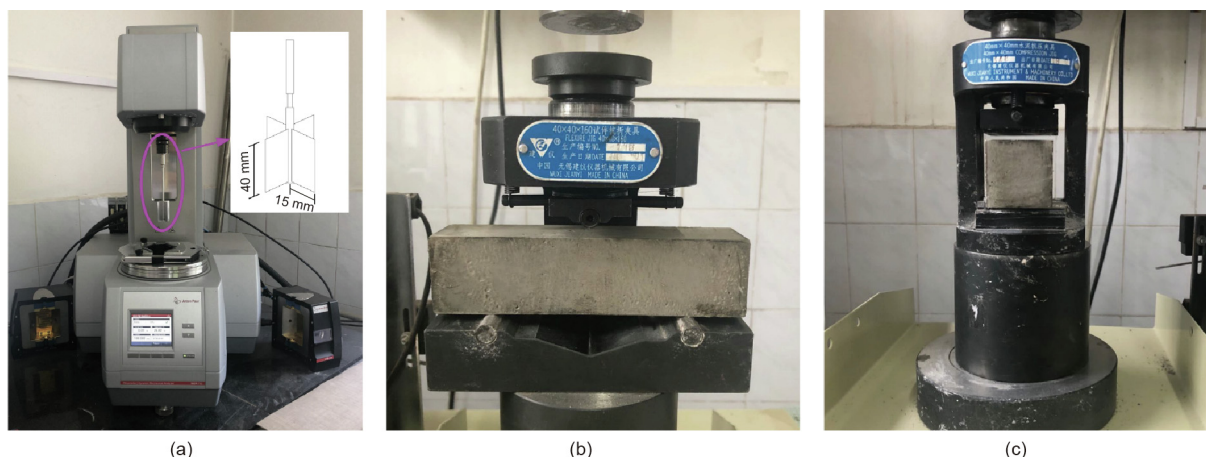


Fig. 4. Rheometer and experiment settings of mechanical property tests: (a) rheological test set; (b) flexural strength test set; and (c) compressive strength test set.

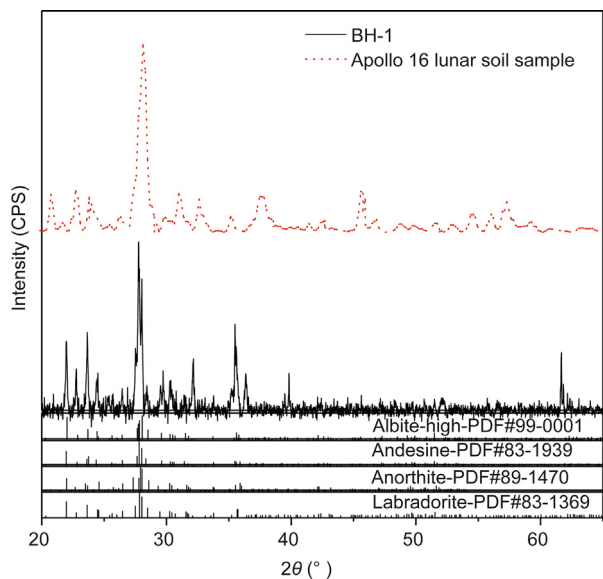


Fig. 5. XRD patterns of BH-1 lunar soil simulant and the Apollo 16 lunar soil sample.

as shown in Fig. 6. This suggests that the reflectance spectrum of the BH-1 lunar regolith simulant is similar to that of the mature mare regolith numbered as 10084 [50].

The morphology of the Apollo lunar regolith sample and raw material (volcanic scoria) of BH-1 lunar regolith simulant measured by SEM shows remarkable similarity, as shown in Fig. 7. Both Apollo lunar regolith samples and the volcanic scoria have a loose and porous micromorphology. The pore size analysis was carried out with the Nano Measurer 1.2 software. It can be observed that the pore size of the real lunar soil is between 21.74 and 60.39 μm. The pore size of the volcanic scoria before milling is between 20.97 and 111.11 μm, which are of the same magnitude as the real lunar soil. It should be noted that the pore structure of volcanic scoria will be destroyed after milling to finer particles. Nevertheless, the similar pore structure and size of volcanic scoria and real lunar soil are still important discoveries for future research, such as when the lunar soil simulant is used to prepare thermal insulation materials with properties that are significantly affected by the pore structure.

Another advantage of BH-1 is its availability for Chinese researchers. Approximately 10 tonnes of BH-1 simulant are currently available for distribution to qualified investigators. The material is stored at Beihang University, Beijing, China. Researchers desiring a portion of this material should address their requests to the corresponding author of this article. Considering that real lunar soil samples are precious and unattainable, BH-1 will facilitate China’s lunar exploration research.

Table 4

Chemical composition (wt%) of JSC-1, CAS-1, DNA-1, and BH-1 lunar soil simulants and real lunar soil collected by Apollo projects.

Item	Apollo 12	Apollo 14	Apollo 15	Apollo 16	JSC-1	CAS-1	DNA-1	BH-1
SiO ₂	42.20	46.30	48.10	46.80	47.71	49.24	47.79	43.3
TiO ₂	7.80	3.00	1.70	1.20	1.59	1.91	1.00	2.9
Al ₂ O ₃	13.60	12.90	17.40	14.60	15.02	15.80	19.16	16.5
FeO	15.30	15.10	10.40	14.30	10.79	11.47	8.75	16.7
MnO	0.20	0.22	0.14	0.19	0.18	0.14	—	0.3
MgO	7.80	9.30	9.40	11.50	9.01	8.72	1.86	3.0
CaO	11.90	10.70	10.70	10.80	10.42	7.52	8.28	8.8
Na ₂ O	0.47	0.54	0.70	0.39	2.70	3.08	4.38	3.8
K ₂ O	0.16	0.31	0.55	0.21	0.82	1.03	3.52	3.3
P ₂ O ₅	0.05	0.40	0.51	0.18	0.66	0.30	—	0.7

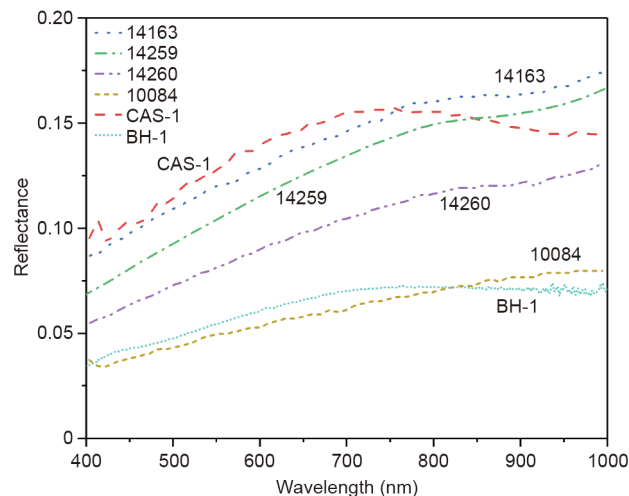


Fig. 6. Reflectance spectra of CAS-1, BH-1 lunar soil simulants, and real lunar soil samples.

The results indicate that the BH-1 lunar soil simulant has a substantial similarity with the real lunar soil in terms of mineral composition, chemical composition, reflectance spectral characteristics, and microscopic morphology. Hence, it is suitable for use as a simulated material for the lunar soil geopolymer reaction.

3.2. Rheological properties of yield stress, flow index, and thinning index

Understanding the rheological properties of mortars is essential to determine their consistency and workability, and therefore, their ease of casting or placement. The effect of alkali activators and different additives on the rheological behavior of the BH-1 pastes was investigated. The variations of shear stress versus shear rate (flow curves) for both ramping up and down periods are shown in Fig. 8. It can be observed that the up ramp curve of BH-1 paste without the alkali activator (blankCg) almost coincides with the down ramp (Cg_down), which means that the shearing action does not have a significant influence on the flow resistance. The addition of an alkali activator and Metamax and Al₂O₃ as additives led the curve to form a thixotropic loop. As shown, the up ramp flow curve (Cg_up) is located above the down ramp, which indicates that the paste of Cg, Al3, Al5, Al10, Kao5, and Kao10 are thixotropic fluids, and the shearing action results in reduced flow resistance. The thixotropic loop area indicated the strength of the thixotropy. The larger the area of the thixotropic loop, the more significant the effect of shear force on fluid structural failure. It can be concluded that BH-1 paste with 10%

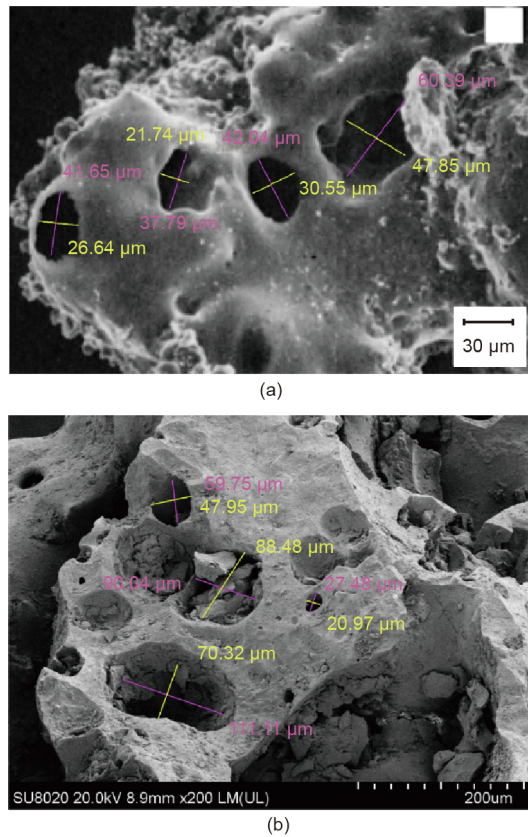


Fig. 7. SEM images and pore size analysis of (a) Apollo lunar soil sample (NASA Photo S87-39605) [30] and (b) source material of BH-1 lunar soil simulant. LM: low magnification; UL: ultra low.

Metamax additive has the maximum thixotropy for the largest thixotropic loop area, as shown in Fig. 8(c).

All the pastes are non-Newtonian fluids, the relationship between shear stress and shear strain rate is nonlinear. The variation of shear stress versus shear rate is indicative of the rheological behavior of materials by the determination of a mathematical rheological model. As seen in Fig. 9, the relationship between shear stress and shear rate $\dot{\gamma}$ in the down ramp curve of alkali-activated BH-1 pastes fits well with the Herschel–Bulkley model (Eq. (1)) with $R^2 > 0.99$, for all test groups.

$$\tau = \tau_0 + k\dot{\gamma}^n \quad (1)$$

where τ , τ_0 , k , and n are the shear stress, yield stress, consistency coefficient, and flow index, respectively. In accordance with the present results, previous studies have demonstrated that geopolymer paste from phosphorus slag activated with sodium silicate solution and NaOH is well adjusted with the Herschel–Bulkley model [37]. The shear TI is calculated by viscosity at a low shear rate to viscosity at a shear rate ten times higher ratio, according to the ASTM D2196-18 standard [47]. The evolution of the TI is obtained using Eq. (2), where H_{10} and H_{100} are the apparent viscosity at the shear speeds of 10 and 100 s^{-1} , respectively. The results of τ_0 , n , and TI are shown in Fig. 9.

$$\text{TI} = \frac{H_{10}}{H_{100}} \quad (2)$$

The yield stress is the minimum shear stress value, above which the material exhibits liquid characteristics, while below it, the material exhibits solid characteristics, according to the prEN ISO 3219-1 standard [52]. For concrete or mortar materials, the yield stress of the material represents the force required to stir the paste.

The higher the yield point, the harder the material is to stir or pump. As shown in Fig. 9, the blankCg paste without alkali activator exhibits the lowest yield stress. The yield stress of the paste increases from 6.79 to 17.00 Pa after the addition of the alkali activator. With the addition of 3% Al_2O_3 , the yield stress continued to increase. The yield stress increases with increasing Al_2O_3 content. The increase in the yield stress value may have been due to the increase in the interaction between the soluble silicate ions of BH-1 and the Na^+ ion content in the activator in Al3/Al5/Al10 paste and more formation of the geopolymer gel. Metamax further improved the yield stress to 157.05 and 269.62 Pa for Kao5 and Kao10, respectively. The amorphous forms of Metamax dissolve faster than Al_2O_3 , leading to more drastic geopolymerization. Another reason why pastes with the addition of Metamax have higher yield stress may be that Metamax has a finer particle size and larger specific surface area compared with that of BH-1 and Al_2O_3 .

The flow index is used to describe the fluid behavior as follows: shear-thinning ($n < 1$), Newtonian fluid ($n = 1$), and shear-thickening ($n > 1$). For shear-thinning fluids, the viscosity decreases with increase in the shear rate, while it increases as the shear rate increases for the shear-thickening fluid. As shown in Fig. 9, the flow indexes for all the test groups were below 1. These resulting BH-1 pastes behaved like a shear-thinning fluid, and decreasing the shear rate led to increased viscosity. It can also be observed that the flow index value was reduced by the alkali activator and Al_2O_3 compared with that of the blankCg, indicating an enhancement of the shear-thinning behavior by the alkali activator and Al_2O_3 . In contrast, Metamax reduced the shear-thinning effect of BH-1 pastes, which was manifested as an increase in the flow index.

The TI is reported by dividing the apparent viscosity at a low rotational speed by the viscosity at a speed ten times higher, as shown in Eq. (2). The resultant viscosity ratio indexes the degree of shear-thinning over that range of rotational speed with higher ratios indicating greater shear thinning. By comparing blankCg and Cg in Fig. 9, it can be observed that the TI value of BH-1 pastes increased after adding the alkali activator, showing stronger shear-thinning behavior. After the addition of Al_2O_3 , the TI value slightly changed. In contrast, Metamax weakened the shear-thinning behavior of mortar, manifested as a decrease in TI.

3.3. Mechanical property analysis

Fig. 10 shows the flexural strength and compressive strength of BH-1 based geopolymer at curing ages of 7 and 28 d. The specimens without extra Al in the Cg group showed the lowest mechanical properties. The 28-day compressive strength was 20.7 MPa, and the flexural strength was 3.8 MPa. As shown in Table 4, the Si/Al ratio of BH-1 is 4.45 which is a typical Al deficient material. Previous study [53] have shown that when the Si/Al ratio of raw material is below 2, sufficient Al element can be provided to participate in the geopolymerization reaction. Because the radius of the Al atom is similar to that of the Si atom, the Al atom can randomly replace the Si atom in the Si and oxygen tetrahedron and connect with the adjacent Si atoms in the form of a corner-sharing oxygen bridge. However, the chemical composition of both BH-1 and real lunar soil contains low alumina, resulting in insufficient Al reactant and weak reactivity.

Both the compressive strength and flexural strength of BH-1 based geopolymer with Al_2O_3 and Metamax added were significantly improved compared with the control group. For flexural strength, when Metamax was added at 10 wt% of BH-1, the maximum flexural strength reached 6.0 MPa for 28 d, which was 57.9% higher than that of the control group. When the Al_2O_3 content was 5 wt%, it reached a maximum value of 5.3 MPa among groups Al3,

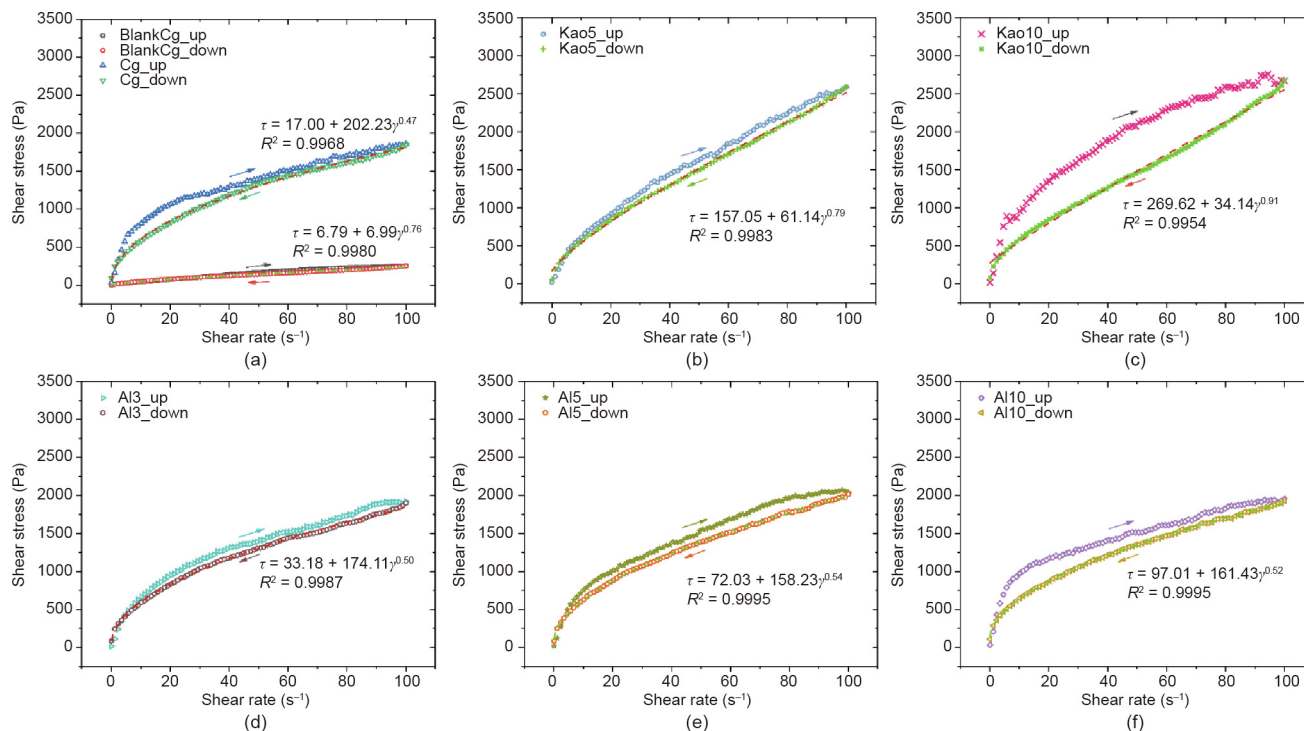


Fig. 8. Flow curves of BH-1 pastes (a) with and without alkali activator and with different additives: (b) 5% Metamax; (c) 10% Metamax; (d) 3% Al₂O₃; (e) 5% Al₂O₃; and (f) 10% Al₂O₃.

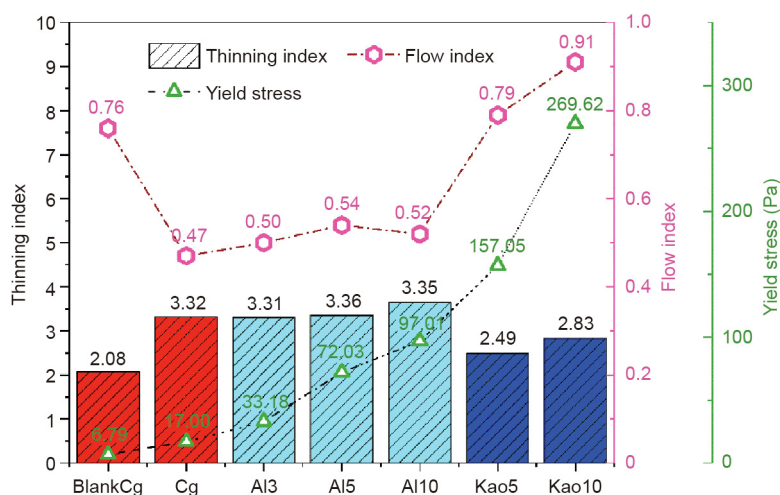


Fig. 9. Rheological parameters of different BH-1 paste.

Al5, and Al10, which was 39.5% higher than that of the control group. Regarding compressive strength, when Al₂O₃ and Metamax were added at 5 wt% of BH-1, the 28-day compressive strength was 45.9% and 78.7% higher than that of the control group. When Al₂O₃ and Metamax were added at 10 wt% of BH-1, the 28-day compressive strength was 46.0% and 100.8% higher than that of the control group. The Al₂O₃ and NaOH solutions reacted as follows: Al₂O₃ + 2NaOH = 2NaAlO₂ + H₂O. The increased AlO₂⁻ ions supplement the reactive Al element, increasing the speed of geopolymerization. The alumina content in Metamax is 46.16% (Table 2), and the Al₂O₃ directly provides the Al source, which supplements the Al element to the mixed system, finally increasing the mechanical strength. It should be noted that the mechanical strength enhancement for adding Metamax is more significant than that for adding Al₂O₃, even though the Al content in Al₂O₃ is higher than that in Metamax

when the same mass is added. This largely stems from the mineral composition and fine particle size of Metamax. The first step of the geopolymer is to dissolve. In an alkaline environment, the chemical bonds of Si–O–Si, Al–O–Al, and Al–O–Si in the raw material are broken to form Si(OH)₄⁻, Al(OH)₄⁻, and Al(OH)₆³⁻ monomers. The amorphous substance is more soluble than the crystalline phase matter. The dominant amorphous substance in the Metamax can quickly dissolve in the alkali system, increasing the concentration of reactants and the reaction rate. Metamax has a relatively small particle size. Most of the reactions occur at the particle–liquid interface. The finer the particle size, the larger the specific surface area, and the stronger the material’s reactivity.

In the construction of a lunar base, the material mass carried from the Earth should be minimized to save space transportation costs. Mass strength efficiency (MSE), labeled as η_m, was defined

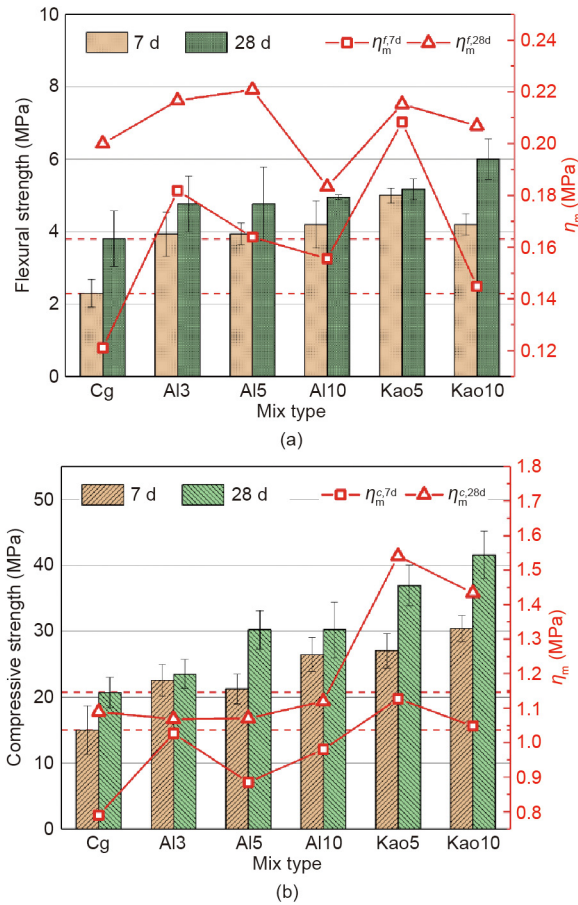


Fig. 10. The 7-day and 28-day (a) flexural strength and (b) compressive strength of geopolymer based on BH-1 lunar soil simulant. η_m : mass strength efficiency; $\eta_m^{f,7d}$ and $\eta_m^{c,7d}$ are the η_m values of the 7-day flexural strength and compressive strength; $\eta_m^{f,28d}$ and $\eta_m^{c,28d}$ are the η_m values of the 28-day flexural strength and compressive strength of each test group.

in Eq. (3) to measure the mass saving effect of the admixture. η_m is the reciprocal of the mass ratio of the sum of the alkali activators and admixtures forming 1 MPa strength to the lunar soil mass. The larger the η_m , the smaller the total mass of the alkaline activator and admixture (Al_2O_3 or Metamax) is to form the unit strength of the BH-1 based geopolymer; thus, less material mass is carried from the Earth.

$$\eta_m = \left[\frac{(m_{SH} + m_{SS} + m_{Al} + m_{Kao}) \times 100}{m_{BH} \times f} \right]^{-1} \quad (3)$$

where f represents flexural strength. Eq. (3) can also be used to calculate the MSE of compressive strength by substituting the value of compressive strength denoted as c .

The flexural strength and compressive strength at a curing age of 7 and 28 days are shown in Fig. 10. It can be observed that the 7-day η_m values are all smaller than that of the 28-day η_m for all test groups, which means that Metamax and Al_2O_3 have a more noticeable effect on the continuous increase in strength. Considering the Moon’s actual application scenarios, the material needs to have high early strength for increasing construction efficiency; therefore, the η_m values of the 7-day flexural strength and 7-day compressive strength of each test group labeled as $\eta_m^{f,7d}$ and $\eta_m^{c,7d}$, respectively, are key evaluation indicators. It can be seen that compared with the control group, which has a $\eta_m^{f,7d}$ of 0.12 MPa and a $\eta_m^{c,7d}$ of 0.79 MPa, the addition of both Al_2O_3 and Metamax increased the value of η_m . Among them, the group with 5% Meta-

max added had the highest η_m value for both flexural strength and compressive strength. The $\eta_m^{f,7d}$ value of Kao5 is 0.21 MPa, which is 75% higher than that of the control group. The $\eta_m^{c,7d}$ of group Kao5 is 1.13 MPa, which is 43% higher than that of the control group. As for the 28-day curing age, the addition of 5% Al_2O_3 and 5% Metamax has the maximum η_m flexural strength and compressive strength, respectively. As shown in Fig. 10(a), the $\eta_m^{f,28d}$ value decreased when the Al_2O_3 content increased to 10% from 5%, even less than that of the control group. The increase in the 28-day flexural strength is also inappreciable at this level. For 28-day compressive strength, the $\eta_m^{c,28d}$ value does not change much with the increase in Al_2O_3 content. Therefore, although the maximum strength is reached when the Al_2O_3 content is 10%, the low η_m indicates dissatisfaction with strength-enhancing efficiency. On the contrary, 5% Al_2O_3 allows a balance between strength enhancement and economic efficiency. From Fig. 10(b), it can be seen that $\eta_m^{c,28d}$ Kao5 is significantly higher than that of other groups. The results above show that 5% addition of Metamax can be used as the best additive among all the test groups. In addition, the enhancement of η_m is also significantly higher than that of previously reported levels. The $\eta_m^{c,7d}$ value of Kao5 in this study is more than 1.5 times that of the geopolymer prepared by Verdolotti et al. [54], using pozzolana from Campi Flegrei sites activated by NaOH and $NaAlO_2$ with a $\eta_m^{c,28d}$ of 0.44 MPa. Djobo et al. [33] obtained a volcanic-ash-based geopolymer with a $\eta_m^{c,28d}$ of 0.93 MPa, which is 20% lower than that of group Kao5 in this study.

3.4. XRD analysis

The XRD patterns of the resulting geopolymer based on BH-1 are shown in Fig. 11. Compared with BH-1, new diffraction peaks appear at 43.3° and 57.4° in the XRD patterns of the resulting geopolymers in groups Al3, Al5, and Al10, which are determined to be incompletely mixed Al_2O_3 by comparison with standard PDF standard cards. For all test groups, new peaks appearing at 21.75° , 28.19° , 33.50° , 38.15° , 42.46° , and 55.05° can be indexed to crystallized calcium aluminosilicate and sodium aluminosilicate. Furthermore, the positions and heights of the diffraction peaks of all the resulting geopolymers are the same as those of

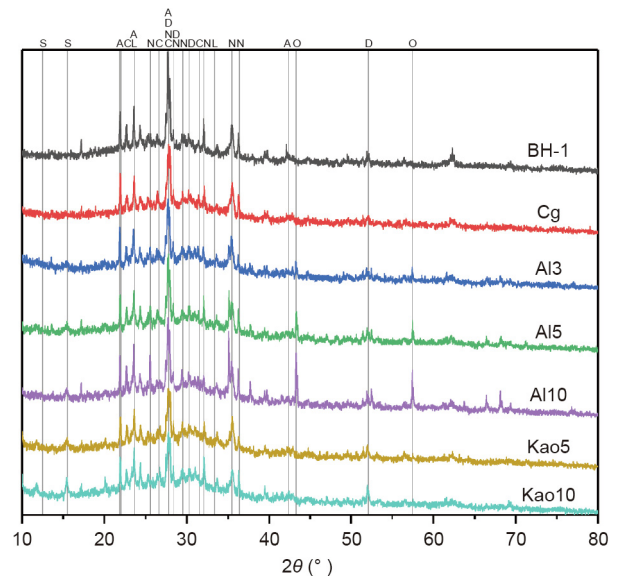


Fig. 11. XRD patterns of BH-1 lunar soil simulant-based geopolymer. A: albite-high; D: andesine; N: anorthite; L: labradorite; C: calcium aluminosilicate; O: alumina.

the raw material BH-1, indicating that the main products of the geopolymerization reaction are amorphous substances. The Kao10 group with the higher mechanical strength has the most apparent background noise and hump peak at 20°–30°. The XRD patterns reveal that crystalline precipitates and chemical precipitation of amorphous structures coincide during geopolymerization. Soluble Ca^{2+} and Na^+ participate in the geopolymerization reaction to form internal crystals with a regular atomic arrangement, which are filled into the cavity of the three-dimensional network structure of the geopolymer, making the structure of the geopolymer more stable and dense [53].

3.5. FTIR analysis

The geopolymer based on BH-1 is an inorganic polymer that can reflect the polymer group's lattice vibration in the infrared spectrum. The FTIR spectra of the BH-1 lunar soil simulant and the resulting geopolymers are depicted in Fig. 12. Some peak features appear in both raw materials, BH-1 and geopolymer products. The wide band with a wavelength between 3434–3447 and 1633–1659 cm^{-1} is the O–H bond stretching vibration peak and H–O–H bond bending vibration peak, which are related to adsorbed atmospheric water and additional water during paste preparation [55]. The water molecule is weakly bound to the geopolymer unit and enveloped in the geopolymer three-dimensional network

structure cavity. The band located at approximately 455–461 cm^{-1} reflects chemically inert Si–O–Si and O–Si–O bonds in a strong alkali environment [56].

The differences between BH-1 and the resulting geopolymers are analyzed as follows. The absorption peak with a wavelength of 1414–1486 cm^{-1} only exists in the resulting geopolymers, which is the stretching vibration peak of the O–C–O bond, indicating that Na_2CO_3 and NaHCO_3 were formed when CO_2 in the air reacted with NaOH in the alkaline activator [57]. The broad and strong peaks of BH-1 at a wavelength of approximately 1004 cm^{-1} are the stretching vibration peaks of Si–O–Si, which shift toward a lower wavelength (985–991 cm^{-1}) after geopolymerization, resulting from the rearrangement of Si–O and Al–O. The original SiO_4 group on the uniform Si–O–Si chain structure in BH-1 is replaced by AlO_4 to form a new amorphous silicoaluminate cementitious phase [57]. This is also confirmed by the XRD analysis in Fig. 5. When the Metamax content was 10%, the shrinkage vibration peak wavelength was the smallest and the strength was the highest, indicating that the polymerization degree was the highest. The corresponding specimens also exhibited the highest mechanical strength.

It should also be noted that absorption peaks appear at wavelengths of 561.55, 670.63, and 754.06 cm^{-1} because of the additional Al_2O_3 and Metamax. Group Kao10 has the largest number of new peaks in this range. These peaks are considered to be Si–O–Si and Al–O–Si symmetric contraction peaks, which may be due to the reaction process of amorphous silicon aluminate in the transformation phase of the semi-crystalline phases, suggesting a higher polymerization degree [56].

3.6. Microstructure and elemental composites analysis through SEM-EDS

The SEM images of the BH-1 lunar soil simulant and the resulting geopolymers are shown in Fig. 13. It can be observed that almost all the particles in BH-1 are smaller than 80 μm in Figs. 13(a) and (b), which is consistent with the particle size analysis results. It can be seen from Figs. 13(c) and (d) that BH-1 presents a bedding structure with sharp edges when magnified at 5.00×10^3 times and 2.00×10^4 times. After the alkali excited reaction without adding extra substances containing aluminum, as shown in Fig. 13(e), the unreacted BH-1 is interlaced with the amorphous gel material generated by geopolymerization. Meanwhile, many cracks are observed. This is due to the insufficient reaction, and the amorphous gel fails to form as a whole, leading to the geopolymer's weakest strength in the Cg group. Fig. 13(f) shows a detailed magnification of the geopolymer in the Cg group. The initial growth of amorphous tissue on the surface of the BH-1 particles can be observed. Figs. 13(g)–(i) show the microscopic morphology of the resulting geopolymers of the three test groups with added Al_2O_3 . It can be observed that after the addition of alumina, the content of newly formed geopolymers with amorphous structure increases with fewer cracks. A further comparison among the three groups shows that the unreacted BH-1 content in group Al3 is the highest, while the morphology difference between groups Al5 and Al10 is insignificant. This further explains that the 28-day strength of group Al10 is less improved than that of group Al5 at the micro-level. Therefore, the amount of Al_2O_3 added should be controlled to ensure the material economy. Figs. 13(j) and (k) are SEM microscope images of Kao5 and Kao10. It can be observed that the amorphous gel has the most complete growth, and therefore, the geopolymer strength is the highest. As the enlarged image in Fig. 13(l) shows, the amorphous gel is a spherical structure formed by the stacking of granular particles.

Fig. 14, Table 5, and Fig. 15 show the microscopic images and elemental analysis results of SEM-EDS. The Si/Al ratio of the

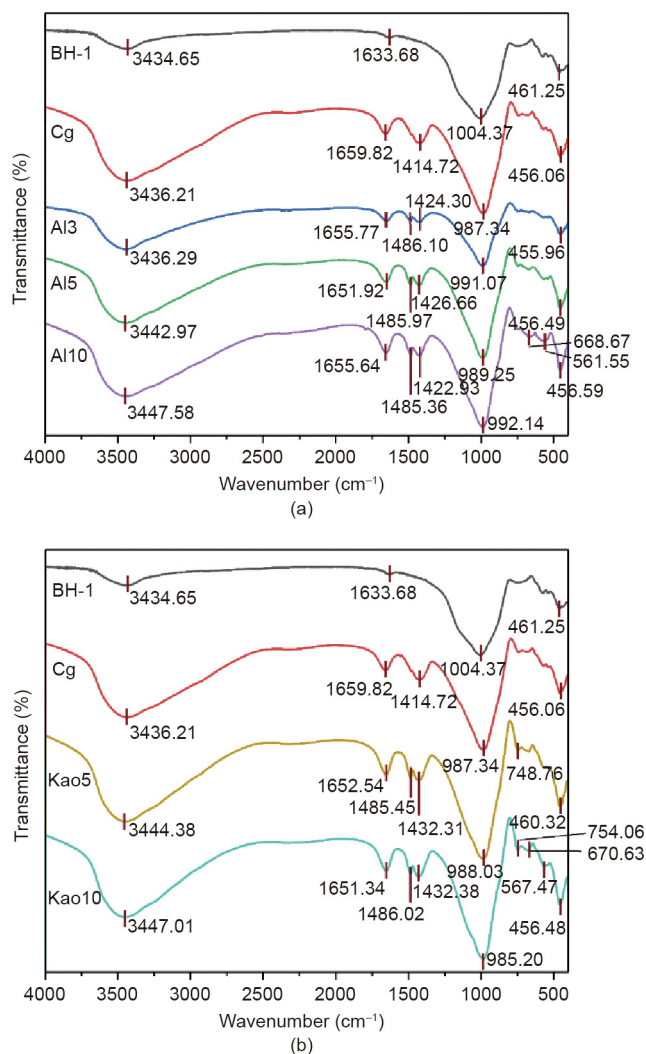


Fig. 12. Infrared spectra of BH-1-based geopolymer: (a) Al_2O_3 test runs; and (b) Metamax test runs.

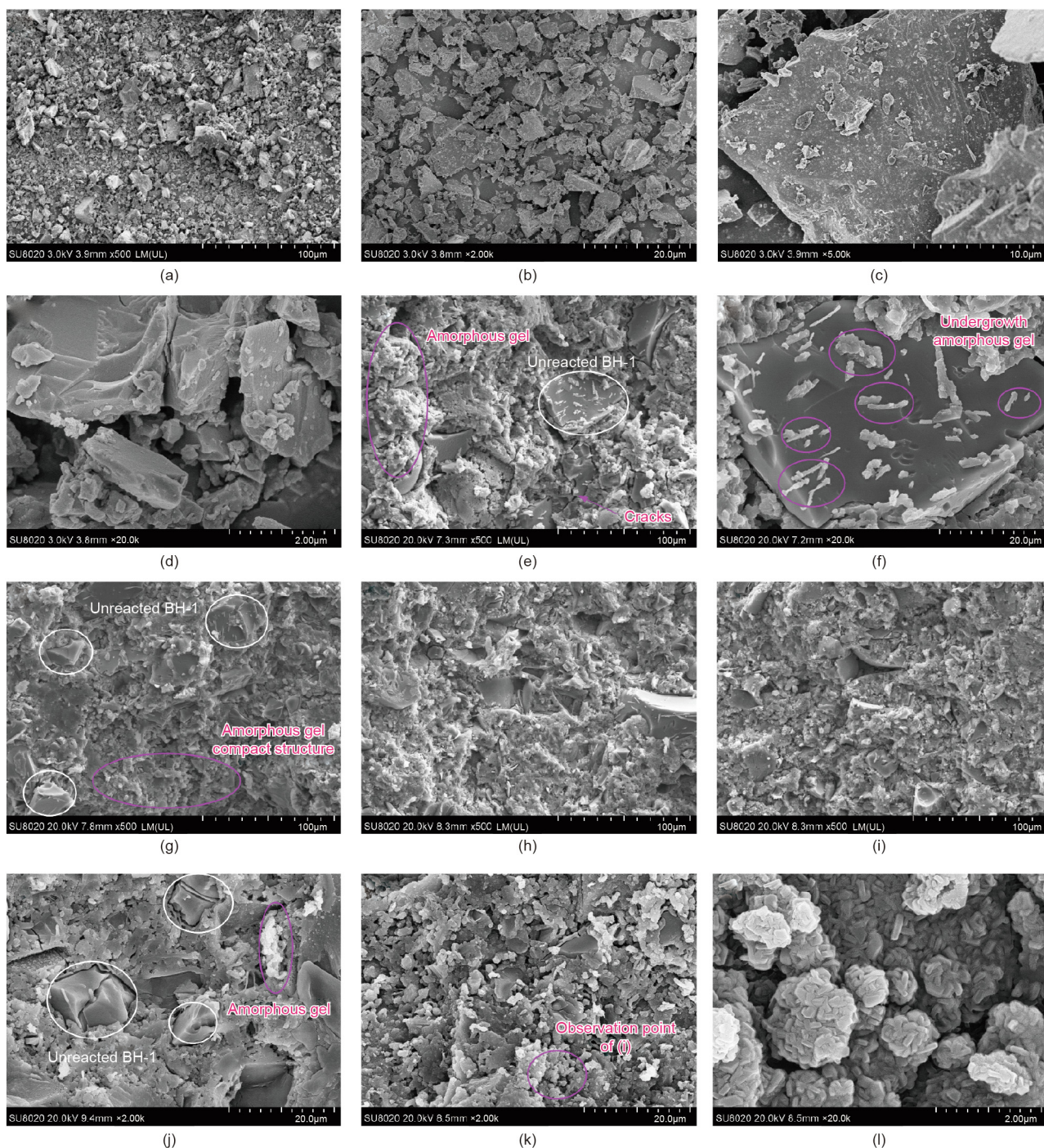


Fig. 13. SEM images of (a)–(d) BH-1 lunar soil simulant under different magnification, (e) resulting geopolymer of Cg, (f) Cg with high magnification, (g) Al3, (h) Al5, (i) Al10, (j) Kao5, (k) Kao10, and (l) Kao10 with high magnification.

amorphous gel in the Cg group is 3.64, lower than that in case of BH-1. In the group with additional Al_2O_3 (Al3, Al5, Al10), it can be seen that with the increase of Al_2O_3 content, the Si/Al ratio decreases, which proves that the Si number substituted by Al in Si–O group increases. Therefore, the silica–aluminum tetrahedral structure becomes more integrated, leading to an increase in mechanical strength. Compared with group Kao5, group Kao10 also shows a decrease in Si/Al ratio and an increase in amorphous gel microstructure. In addition, the sodium–silicon ratio (Na/Si) in each experimental group is improved compared with that in the control group, indicating that Na is also involved in the reaction,

and its possible role is to neutralize the negative charge of the tetrahedral structure [53].

3.7. Geopolymerization analysis of chemical bonds through ^{27}Al MAS-NMR

The amorphous structure of the resulting geopolymer based on BH-1 was analyzed by NMR ^{27}Al spectrum analysis. The chemical displacements of Al denoted as δ indicate the chemical environment of the Al atoms. As shown in Fig. 16, there is a distinct resonance peak at 60 ppm (parts per million), which corresponds to the

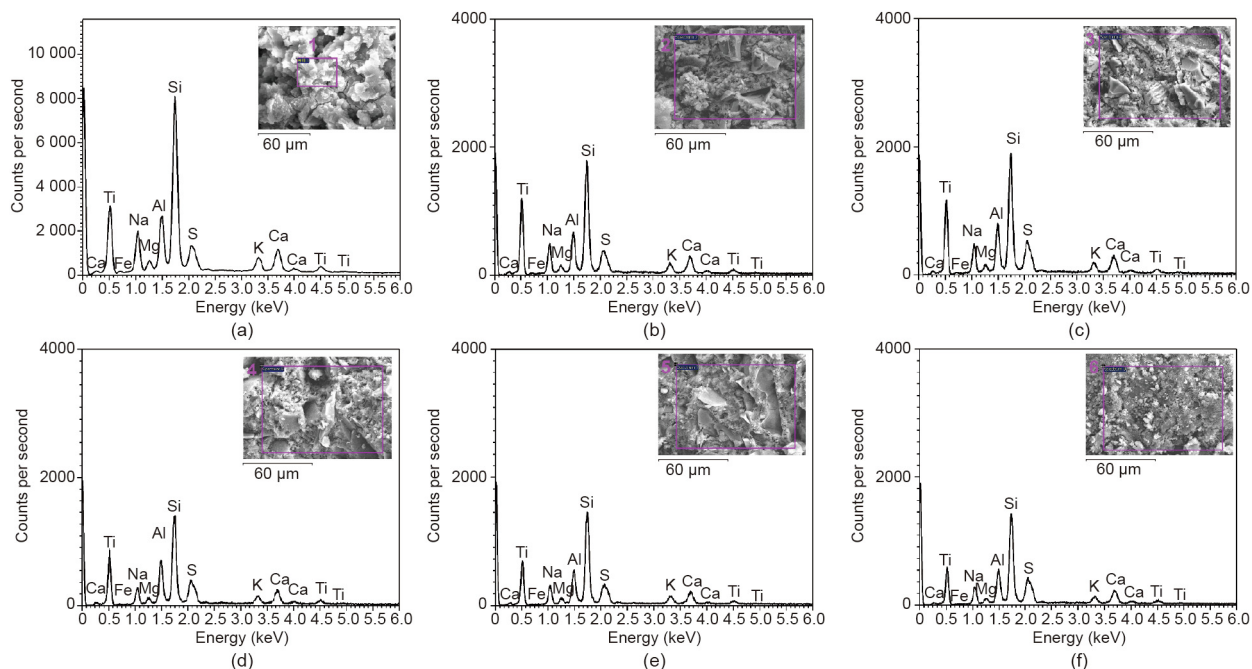


Fig. 14. SEM images and EDS analysis of BH-1 based geopolymers: (a) Cg, (b) Al3, (c) Al5, (d) Al10, (e) Kao5, and (f) Kao10.

Table 5
The average elemental component results of representative EDS spectra from Fig. 14.

Location in Fig. 14	Elemental component (at%)						
	Na	Mg	Al	Si	Ca	Ti	Fe
1	17.18	3.56	13.52	49.21	6.03	1.63	8.89
2	18.26	3.20	14.59	47.42	6.51	1.61	8.39
3	16.72	3.26	15.93	48.01	6.33	1.56	8.19
4	12.54	3.36	19.18	47.19	6.53	1.83	9.38
5	14.97	3.31	15.12	49.64	5.77	1.74	9.44
6	14.13	2.78	15.89	49.54	6.76	1.85	9.04

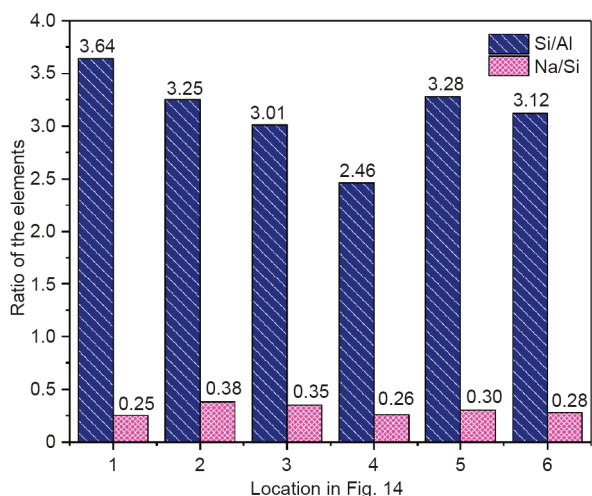


Fig. 15. The ratio of elements of different resulting geopolymers analyzed by EDS tests.

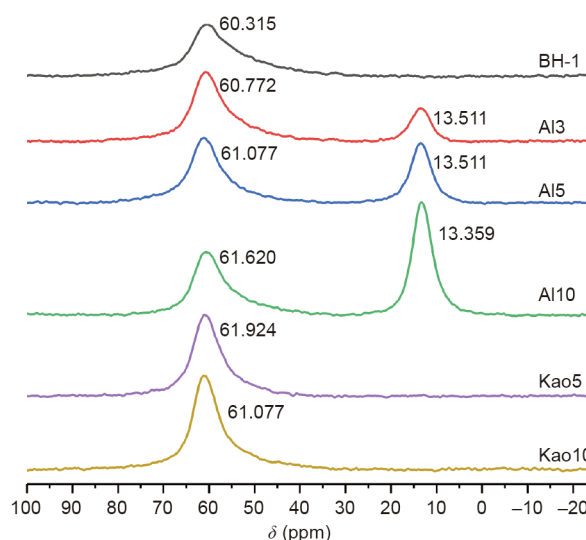


Fig. 16. ²⁷Al MAS-NMR spectra of BH-1 lunar soil simulants based geopolymers.

Al in the tetrahedral structure, resulting from the rearrangement of the electron cloud around the Al atom after replacing the Si atoms in the original SiO₄ tetrahedral structure [58], which corresponds to the absorption peak of 985–991 cm⁻¹ in the previous FTIR analysis. In addition, with the increase in the content of Al₂O₃ and

Metamax, the peak intensity also increases, indicating that more Al atoms enter the tetrahedral structure instead of Si [59]. At the same time, the mechanical strength of the geopolymers increases. In addition, formant peaks were observed in groups Al3, Al5, and Al10 at 13 ppm, which corresponds to Al atoms in unreacted Al₂O₃.

4. Conclusions and future work

In this study, a new type of lunar soil simulant named BH-1 was prepared based on the volcanic scoria of Jinlongdingzi in Jilin Province, China. Geopolymers were prepared from BH-1, providing a theoretical and experimental basis for the production of pavement materials by the *in situ* polymerization reaction of lunar soil on the Moon. Through mechanical properties testing rheological behavior analysis and microstructure analysis of BH-1 and the resulting geopolymer products, the following conclusions were obtained:

(1) A new BH-1 lunar soil simulant was prepared from volcanic ash. BH-1 was compared with Apollo lunar soil and other simulated lunar soil through XRD, XRF, reflection spectrum, and SEM tests. The results show that BH-1 has a high similarity with real lunar soil in terms of mineral and chemical composition, reflected light characteristics, and microscopic morphology. The preparation methods and characterization of geopolymers based on BH-1 are substitutable for synthesis of geopolymers with real lunar soil.

(2) The BH-1 pastes activated with NaOH and sodium silicate as a thixotropic fluid behaved like a shear-thinning fluid. Their rheological behavior fit well with the Herschel–Bulkeley model. The addition of Al_2O_3 improved the yield stress of the BH-1 paste, reduced the flow index, and had little impact on the TI. The addition of Metamax improved the yield stress and flow index of BH-1 paste and reduced the TI.

(3) The addition of Al_2O_3 and Metamax can effectively improve the mechanical strength of geopolymers based on BH-1. The 28-day maximum compressive strength can be increased by more than 100%. Meanwhile, the index of “mass strength efficiency,” labeled as η_m , was developed to evaluate the improving effect of unit mass Al_2O_3 and Metamax on the mechanical strength of geopolymer. The results show that the addition of both Al_2O_3 and Metamax can significantly improve its value η_m , thus effectively reducing the material transportation cost. The addition of 5% Metamax reaches the balance between the increased effect of η_m and economy efficiency.

(4) The addition of Al_2O_3 and Metamax to BH-1 facilitates the dissolution of alumina species, consequently promoting the $Si(OH)_4^-$, $Al(OH)_4^-$ and $Al(OH)_6^{3-}$ monomers contents in geopolymer pastes. Polycondensation and the formation of silicon aluminum tetrahedron binder are promoted, which increases the mechanical strength.

(5) Metamax has a more noticeable effect on improving the mechanical strength of the BH-1 geopolymer. The increasing effect mechanism is attributed to the abundant Al source, small particle size (large specific surface area), and abundant soluble amorphous mineral structure of Metamax.

Despite the limitations of the finer particle size of BH-1 compared with real lunar soil, the study certainly adds to the understanding of the feasibility of preparing high-strength geopolymers with BH-1 lunar soil simulant and, at the same time, to improve mechanical properties to save space transportation cost by adding Al_2O_3 and Metamax. To further improve the Moon transportation infrastructure construction, the preparation and characterization of the BH-1 geopolymer under vacuum, high-and-low-temperature cycling, and low-gravity conditions should be further explored.

Acknowledgments

This research was supported by the National Key Research and Development (R&D) Program of China (2018YFB1600100), National Natural Science Foundation of China (51978029 and 51622805), and Shanghai Pujiang Program. The authors also acknowledge NASA/Lunar and Planetary Institute for permission

of the figures in “Lunar sourcebook: a user's guide to the moon” to be reused in this study.

Compliance with ethics guidelines

Siqi Zhou, Chenghong Lu, Xingyi Zhu, and Feng Li declare that they have no conflict of interest or financial conflicts to disclose.

References

- [1] Wang C, Nie H, Chen J, Lee HP. The design and dynamic analysis of a lunar lander with semi-active control. *Acta Astronaut* 2019;157:145–56.
- [2] Dalton C, Hohmann E. Conceptual design of a lunar colony. Technical reports. Texas: National Aeronautics and Space Administration (NASA)/ American Society for Engineering Education (ASEE) Systems Design Institute; 1972.
- [3] Zheng Y, Ouyang Z, Li C, Liu J, Zou Y. China's lunar exploration program: present and future. *Planet Space Sci* 2008;56(7):881–6.
- [4] Vaniman D, Reedy R, Heiken G, Olhoeft G, Mendell W. The lunar environment. In: Heiken G, Vaniman D, French BM, editors. *Lunar sourcebook: a user's guide to the moon*. New York: Cambridge University Press; 1991. p. 27–60.
- [5] Davis G, Montes C, Eklund S. Preparation of lunar regolith based geopolymer cement under heat and vacuum. *Adv Space Res* 2017;59(7):1872–85.
- [6] Brandenburg B. Lunar rover on the moon [Internet]. Utah: Bryan Brandenburg; 2013 Mar 17 [cited 2020 Jun 9]. Available from: <http://bryanmbrandenburg.com/lunar-rover-on-moon/>.
- [7] Lunar rover Yutu travels an average of 200 meters per hour [Internet]. Hong Kong: Phoenix New Media; 2013 Dec 16 [cited 2020 Jun 9]. Available from: http://news.ifeng.com/mainland/special/changsanhaohao/content-3/detail_2013_12/16/32145473_0.shtml?_114sobiaoqian. Chinese.
- [8] Dominguez JA, Whitlow J. Upwards migration phenomenon on molten lunar regolith: new challenges and prospects for ISRU. *Adv Space Res* 2019;63(7):2220–8.
- [9] Winkless L. Moon dust: a building material for a lunar base? *Mater Today* 2015;18(4):181.
- [10] Anand M, Crawford LA, Balat-Pichelin M, Abanades S, van Westrenen W, Peraudeau G, et al. A brief review of chemical and mineralogical resources on the Moon and likely initial *in situ* resource utilization (ISRU) applications. *Planet Space Sci* 2012;74(1):42–8.
- [11] Khoshnevis B, Yuan X, Zahir B, Zhang J, Xia B. Construction by contour crafting using sulfur concrete with planetary applications. *Rapid Prototyping J* 2016;22(5):848–56.
- [12] Montes C, Broussard K, Congre M, Simicevic N, Mejia J, Tham J, et al. Evaluation of lunar regolith geopolymer binder as a radioactive shielding material for space exploration applications. *Adv Space Res* 2015;56(6):1212–21.
- [13] Wilhelm S, Curbach M. Review of possible mineral materials and production techniques for a building material on the moon. *Struct Concr* 2014;15(3):419–28.
- [14] Taylor SL, Jakus AE, Koube KD, Ibeh AJ, Geisendorfer NR, Shah RN, et al. Sintering of micro-trusses created by extrusion-3D-printing of lunar regolith inks. *Acta Astronaut* 2018;143:1–8.
- [15] Taylor LA, Pieters CM, Britt D. Evaluations of lunar regolith simulants. *Planet Space Sci* 2016;126:1–7.
- [16] McKay DS, Carter JL, Boles WW, Allen CC, Allton JH. JSC-1: a new lunar regolith simulant. In: *Proceedings of the 24th Lunar and Planetary Science Conference*; 1993 Mar 15–19; Houston, TX, USA; 1993.
- [17] Hill E, Patchen AD, Taylor L, Day J, Day JMD. Supplement, quantitative characterization of JSC-1 and MLS-1 lunar soil simulants. In: *Proceedings of 68th Annual Meeting of the Meteoritical Society*; 2005 Sep 12–16; Gatlinburg, TN, USA; 2005.
- [18] Zheng Y, Wang S, Ouyang Z, Zou Y, Liu J, Li C, et al. CAS-1 lunar soil simulant. *Adv Space Res* 2009;43(3):448–54.
- [19] Ray CS, Reis ST, Sen S, O'Dell JS. JSC-1A lunar soil simulant: characterization, glass formation, and selected glass properties. *J Non-Cryst Solids* 2010;356(44–49):2369–74.
- [20] Ryu BH, Wang CC, Chang L. Development and geotechnical engineering properties of KLS-1 lunar simulant. *J Aerosp Eng* 2018;31(1):04017083.
- [21] Davidovits J. Geopolymers and geopolymeric materials. *J Therm Anal* 1989;35(2):429–41.
- [22] Chindaprasirt P, Chareerat T, Hatanaka S, Cao T. High-strength geopolymer using fine high-calcium fly ash. *J Mater Civ Eng* 2011;23(3):264–70.
- [23] Zhang Z, Provis JL, Reid A, Wang H. Mechanical, thermal insulation, thermal resistance and acoustic absorption properties of geopolymer foam concrete. *Cem Concr Res* 2015;62:97–105.
- [24] Slavik R, Bednarik V, Vondruska M, Nemecek A. Preparation of geopolymer from fluidized bed combustion bottom ash. *J Mater Process Technol* 2008;200(1–3):265–70.
- [25] Wang A, Zheng Y, Zhang Z, Liu K, Li Y, Shi L, et al. The durability of alkali-activated materials in comparison with ordinary portland cements and concretes: a review. *Engineering* 2020;6(6):695–706.
- [26] Wallah SE. Drying shrinkage of heat-cured fly ash-based geopolymer concrete. *Mod Appl Sci* 2009;3(12):14–21.
- [27] Anand M. Lunar water: a brief review. *Earth Moon Planets* 2010;107(1):65–73.

- [28] Wang KT, Lemougna PN, Tang Q, Li W, Cui XM. Lunar regolith can allow the synthesis of cement materials with near-zero water consumption. *Gondwana Res* 2017;44:1–6.
- [29] Pilehvar S, Arnhof M, Pamies R, Valentini L, Kjøniksen AL. Utilization of urea as an accessible superplasticizer on the moon for lunar geopolymer mixtures. *J Clean Prod* 2020;247:119177.
- [30] Mckay DS, Heiken G, Basu A, Blanford G, Simon S, Reedy R, et al. *Lunar sourcebook: a user's guide to the moon*. New York: Cambridge University Press; 1991. p. 305–6.
- [31] Li Z, Gong J, Du S, Wu J, Li J, Hoffman D, et al. Nano-montmorillonite modified foamed paste with a high volume fly ash binder. *RSC Adv* 2017;7(16):9803–12.
- [32] Tchakoute Kouamo H, Elimbi A, Mbey JA, Ngally Sabouang CJ, Njopwouo D. The effect of adding alumina-oxide to metakaolin and volcanic ash on geopolymer products: a comparative study. *Constr Build Mater* 2012;35:960–9.
- [33] Djobo JNY, Elimbi A, Tchakouté HK, Kumar S. Volcanic ash-based geopolymer cements/concretes: the current state of the art and perspectives. *Environ Sci Pollut Res Int* 2017;24(5):4433–46.
- [34] Barnes HA, Barnes JF, Walters K. *An introduction to rheology*. Amsterdam: Elsevier; 1989.
- [35] Zhang Y, Zhang Y, She W, Yang L, Liu G, Yang Y. Rheological and harden properties of the high-thixotropy 3D printing concrete. *Constr Build Mater* 2019;201:278–85.
- [36] Panda B, Tan MJ. Rheological behavior of high volume fly ash mixtures containing micro silica for digital construction application. *Mater Lett* 2019;237:348–51.
- [37] Hamideh M, Ebrahim NK, Sanchez AP, Fernandez-Jimenez A. Rheology of activated phosphorus slag with lime and alkaline salts. *Cem Concr Res* 2018;113:121–9.
- [38] Poulesquen A, Frizon F, Lambertin D. Rheological behavior of alkali-activated metakaolin during geopolymerization. *J Non-Cryst Solids* 2011;357(21):3565–71.
- [39] Wallevik OH, Feys D, Wallevik JE, Khayat KH. Avoiding inaccurate interpretations of rheological measurements for cement-based materials. *Cem Concr Res* 2015;78(Pt A):100–9.
- [40] Aiad I. Influence of time addition of superplasticizers on the rheological properties of fresh cement pastes. *Cem Concr Res* 2003;33(8):1229–34.
- [41] Yahia A, Khayat KH. Applicability of rheological models to high-performance grouts containing supplementary cementitious materials and viscosity enhancing admixture. *Mater Struct* 2003;36(6):402–12.
- [42] Peng J, Deng D, Liu Z, Yuan Q, Ye T. Rheological models for fresh cement asphalt paste. *Constr Build Mater* 2014;71:254–62.
- [43] Djobo JNY, Tchadjé LN, Tchakouté HK, Kenne BBD, Elimbi A, Njopwouo D, et al. Synthesis of geopolymer composites from a mixture of volcanic scoria and metakaolin. *J Asian Ceram Soc* 2014;2(4):387–98.
- [44] Alexiadis A, Alberini F, Meyer ME. Geopolymers from lunar and Martian soil simulants. *Adv Space Res* 2017;59(1):490–5.
- [45] Slyuta EN. Physical and mechanical properties of the lunar soil (a review). *Sol Syst Res* 2014;48(5):330–53.
- [46] Zhou S, Zhu X, Lu C, Li F. Synthesis and characterization of geopolymer from lunar regolith simulant based on natural volcanic scoria. *Chin J Aeronaut*. In press.
- [47] ASTM D2196-18e1: Standard test methods for rheological properties of non-newtonian materials by rotational viscometer. ASTM standard. West Conshohocken: ASTM International; 2018.
- [48] Williams JP, Paige DA, Greenhagen BT, Sefton-Nash E. The global surface temperatures of the Moon as measured by the Diviner Lunar Radiometer Experiment. *Icarus* 2017;283:300–25.
- [49] Gates-Rector S, Blanton T. The Powder Diffraction File: a quality materials characterization database. *Powder Diffr* 2019;34(4):352–60.
- [50] Robens E, Bischoff A, Schreiber A, Unger KK. Investigation of surface properties of lunar regolith part III. *J Therm Anal Calorim* 2008;94(3):627–31.
- [51] Li C, Xie K, Liu A, Shi Z. The preparation and characterization of NEU-1 lunar soil simulants. *JOM* 2019;71(4):1471–6.
- [52] PrEN ISO 3219-1: Plastics—polymers/resins in the liquid state or as emulsions or dispersions—determination of viscosity using a rotational viscometer with defined shear rate ISO/TC 35/SC 9 general test methods for paints and varnishes. Geneva: International Organization for Standardization; 1993.
- [53] Shi C, Fernández-Jiménez A, Palomo A. New cements for the 21st century: the pursuit of an alternative to Portland cement. *Cem Concr Res* 2011;41(7):750–63.
- [54] Verdolotti L, Iannace S, Lavorgna M, Lamanna R. Geopolymerization reaction to consolidate incoherent pozzolanic soil. *J Mater Sci* 2008;43(3):865–73.
- [55] Fernández-Jiménez A, Palomo A. Composition and microstructure of alkali activated fly ash binder: effect of the activator. *Cem Concr Res* 2005;35(10):1984–92.
- [56] Zhang Y, Sun W, Li Z. Composition design and microstructural characterization of calcined kaolin-based geopolymer cement. *Appl Clay Sci* 2010;47(3–4):271–5.
- [57] Tchakouté HK, Kong S, Djobo JNY, Tchadjé LN, Njopwouo D. A comparative study of two methods to produce geopolymer composites from volcanic scoria and the role of structural water contained in the volcanic scoria on its reactivity. *Ceram Int* 2015;41(10):12568–77.
- [58] Zhang M, Zhao M, Zhang G, El-Korchi T, Tao M. A multiscale investigation of reaction kinetics, phase formation, and mechanical properties of metakaolin geopolymers. *Cement Concr Compos* 2017;78:21–32.
- [59] Djobo JNY, Elimbi A, Tchakouté HK, Kumar S. Reactivity of volcanic ash in alkaline medium, microstructural and strength characteristics of resulting geopolymers under different synthesis conditions. *J Mater Sci Technol* 2016;51(22):10301–17.